A Combination of Two Visible-Light Responsive Photocatalysts for Achieving the Z-Scheme in the Solid State

Hyeong Jin Yun,[†] Hyunjoo Lee,[‡] Nam Dong Kim,[†] David Minzae Lee,[†] Sungju Yu,[†] and Jongheop Yi[†,*]

[†]World Class University Program of Chemical Convergence for Energy & Environment, Institute of Chemical Processes, School of Chemical and Biological Engineering, Seoul National University, Seoul 151-741, Republic of Korea, and [‡]Department of Chemical and Biomolecular Engineering, Yonsei University, Seoul 120-749, Republic of Korea

ABSTRACT The light reaction in natural photosynthesis is generally recognized as one of the most efficient mechanisms for converting solar energy into other energy sources. We report herein on a novel strategy for generating H_2 fuel *via* an artificial Z-scheme mechanism by mimicking the natural photosynthesis that occurs in green plants. Designing a desirable photocatalyst by mimicking the Z-scheme mechanism leads to a conduction band that is sufficiently high to reduce protons, thus decreasing the probability of charge recombination. We combined two visible light sensitive photocatalysts, CdS and carbon-doped TiO_2, with different band structures. The used of this combination, that is, CdS/Au/$TiO_{1.96}C_{0.04}$, resulted in the successful transfer of photogenerated electrons to a higher energy level in the form of the letter `Z'. The system produced about a 4 times higher amount of H_2 under irradiation by visible light than CdS/Au/TiO_2. The findings reported herein describe an innovative route to harvesting energy by mimicking natural photosynthesis, and is independent of fossil fuels.

KEYWORDS: photocatalysis · artificial photosynthesis · hydrogen · solid-state · z-scheme · water-splitting

Since the effective conversion of solar energy into useful energy forms has the potential for achieving an environmental friendly society, it is not surprising that numerous attempts have been made to directly utilize solar energy in the form of solar cells.[1−4] Such attempts involved the photocatalytic production of hydrogen, for use as a fuel, *via* water-splitting,[5−18] and related techniques.[19−25] In particular, photocatalytic water-splitting has attracted considerable interest as a green energy resource, due to the environmental and economic superiority of solar and hydrogen energy. Among the reported techniques,[5−18] biomimetic artificial photosynthesis represents an appealing strategy for generating large amounts of hydrogen fuel *via* water-splitting because it permits photogenerated electrons to be transferred to a higher energy level under irradiation by solar light with a low photon energy.[17,18] In green plants, the reduction of protons is accomplished by transferring photoinduced electrons to reactants in a manner analogous to the so-called Z-scheme mechanism of the light reaction in the natural photosynthesis system[26,27] (Scheme 1a). PS II initially oxidizes water with electrons and subsequently activates them to achieve a higher potential. Then, they move to PS I through a complex charge-transfer chain. Transferred electrons are activated again at PS I with a sufficiently high potential to produce ATP and NADPH. When passing through other complex charge-transfer chains, they are used to synthesize ATP and NADPH with the reduction of protons. In biomimetic water-splitting, two types of photocatalysts with different band structures could be used as substitutes for PS I and II, respectively. The electrons that are photogenerated by PS II are transferred to the valence band of PS I. These electrons then recombine with holes photogenerated at PS I. The electrons that are excited at PS I then have a sufficiently high potential for proton reduction. By taking advantage of a combination of PS I and PS II, the probabilities of charge recombination would be decreased significantly, thus resulting in more electrons available to participate in the reduction step of the reaction.

It is usually difficult to generate high levels of H_2 in biomimetic photocatalytic water-splitting techniques consisting of isolated photosystems and redox mediators (Ox/Red)[17,18] because the Ox and Red mobile components in solution compete with the redox reactions of PS I and PS II, respectively.[28] The solid state Z-scheme, in

* Address correspondence to jyi@snu.ac.kr.

Received for review February 18, 2011 and accepted April 18, 2011.

Published online April 18, 2011
10.1021/nn2006738

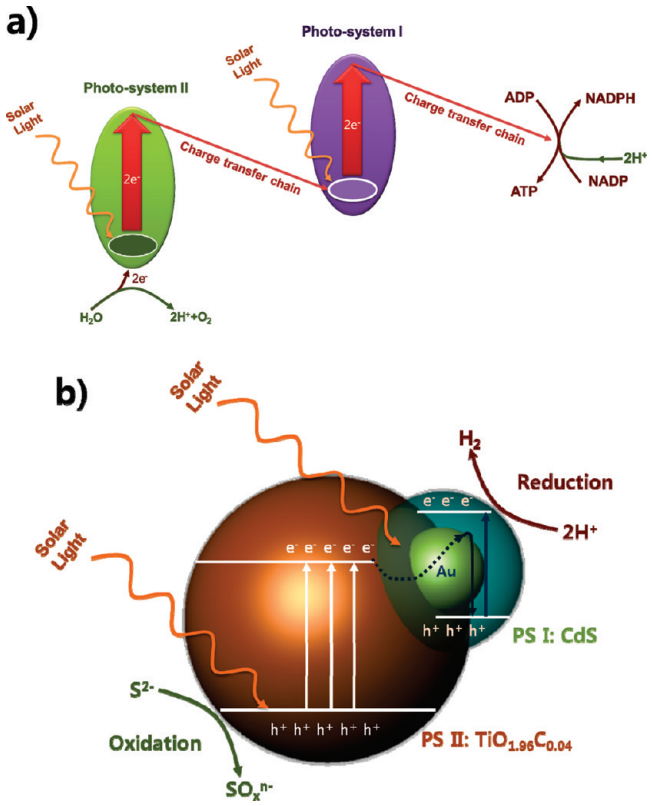

Scheme 1. Z-scheme mechanisms in the natural and artificial photosynthesis system: (a) light reaction in natural photosynthesis system; (b) CdS/Au/$TiO_{1.96}C_{0.04}$ designed to mimic the natural photosynthesis system.

which semiconductors with different levels of band gap energy E_g, for example, CdS and TiO_2 are utilized without any intermediates, has been proposed.[28] This system, however, cannot be considered to be a bona fide Z-scheme under irradiation by visible light because bare TiO_2 can only generate electrons when irradiated with UV light.[28] Thus, an actual biomimetic Z-scheme should consist of materials that produce the desired products when irradiated with visible light.

In the present study, we first combined visible light-responsive photocatalysts, carbon-doped titania ($TiO_{2-x}C_x$, where x denotes the molar ratio of carbon dopant) and CdS, in a nanoparticulate system to achieve a Z-scheme mechanism in the solid state. We previously developed a facile route for the synthesis of large amounts of $TiO_{2-x}C_x$ nanoparticles with a uniform size and shape by wet chemistry. The synthesized $TiO_{2-x}C_x$ nanoparticles were found to effectively function as a visible light sensitive photocatalyst.[29,30] The optimal oxidative photocatalytic performance was observed when 4 atomic % carbon was incorporated into the anatase framework of TiO_2 ($TiO_{1.96}C_{0.04}$).[30] Because the photocatalyst used in PS II in biomimetic water-splitting should function as a strong oxidant when irradiated with visible light, $TiO_{1.96}C_{0.04}$ with a E_g of 2.6 eV has the characteristics for serving as an appropriate material for PS II. To determine whether $TiO_{1.96}C_{0.04}$ is a appropriate material for use as a substitute for PS II, the photocatalytic oxidation of the S^{2-} anion was performed under irradiation by visible light (see Supporting Information, Figure S1). The photocatalytic oxidative performance of $TiO_{1.96}C_{0.04}$ was superior to that for TiO_2 (commercially available P25 and anatase). In addition, it is well-known that the conduction band of CdS has a sufficiently high energy level to reduce protons to H_2 under irradiation by visible light. Thus, an artificial photosynthesis system, in a nanoparticulate form, should be feasible using a combination of $TiO_{1.96}C_{0.04}$ and CdS as shown in Scheme 1b. Irradiation by visible light can induce the delocalization of charges at $TiO_{1.96}C_{0.04}$ as well as CdS. The photogenerated electrons at PS II move to the valence band of CdS through a Au core, and then recombine with photogenerated holes at the CdS. As a result, the lifetime of photogenerated electrons at PS I, which have a sufficiently high reducing power to generate hydrogen molecules, becomes longer due to the lower probability of their recombination. This realization of a biomimetic Z-scheme charge transfer mechanism permits higher amounts of hydrogen fuel to be generated than can be achieved by a typical sensitizing technique under irradiation by visible light. In addition, the presence of a Au core with a large work function leads to an increase in charge separation efficiency.[28] Thus, it would be expected that a CdS/Au/$TiO_{1.96}C_{0.04}$ heterojunction

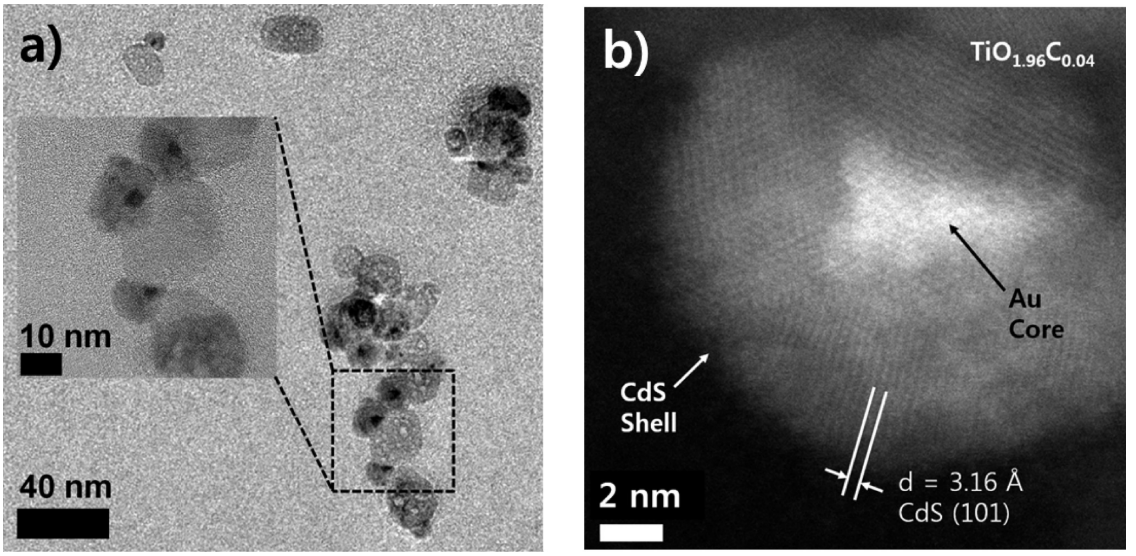

Figure 1. Morphological structure of $CdS/Au/TiO_{1.96}C_{0.04}$ nanoparticle. (a) TEM image of the synthesized $CdS/Au/TiO_{1.96}C_{0.04}$ nanoparticle. (b) HAADF-STEM image of synthesized $CdS/Au/TiO_{1.96}C_{0.04}$ nanoparticles. It can be seen that a hemispherical Au@CdS core−shell structure was formed on the $TiO_{1.96}C_{0.04}$. Interplanar distances shell (3.16 Å) indicates the successful production of wurtzite-structured CdS.

photocatalyst would have the potential to produce large amounts of H_2 fuel *via* the conversion of solar light energy.

RESULTS AND DISCUSSION

$TiO_{1.96}C_{0.04}$ nanoparticles were prepared *via* a dissolution-recrystallization process from a highly viscous $Ti(OH)_4$ gel in the presence of oleic acid. Carbon-doping was accomplished *via* the adsorption of carboxylic groups from oleic acid to the TiO_2 seed materials. Au nanoparticles were deposited on the surface of $TiO_{1.96}C_{0.04}$ by the direct reduction of $AuCl^{4-}$ using $NaBH_4$, a strong reducing agent. As previously reported,[28] a hemispherical Au@CdS core−shell structure can be formed on $TiO_{1.96}C_{0.04}$ a photodeposition process, after rigorously stirring an ethanol suspension containing $Au/TiO_{1.96}C_{0.04}$, sulfur, and Cd^{2+}. Large amounts of sulfur molecules are adsorbed on the surface of a Au nanoparticle deposited on $TiO_{1.96}C_{0.04}$ due to their great affinity for Au. When UV light is used to irradiate the prepared suspension, the sulfur is reduced to S^{2-} which instantly reacts with Cd^{2+} to form a CdS shell. Using this procedure, it is possible to selectively deposit CdS on the surface of Au, with the resulting formation of a hemispherical Au@CdS core−shell structure on $TiO_{1.96}C_{0.04}$ (Figure 1). The diameter of the deposited Au core is between 4 and 6 nm, and the thickness of the CdS shell is in the range of 5 to 10 nm. The lattice arrays of the shell show interplanar distances corresponding to [101] of CdS, indicating the successful development of a wurtzite-structured CdS.

The formation of CdS was also verified in X-ray diffraction (Figure 2) and ultraviolet−visible light diffused reflectance spectroscopy (UV−vis−DRS) experiments (Figure 5). The prepared $TiO_{1.96}C_{0.04}$

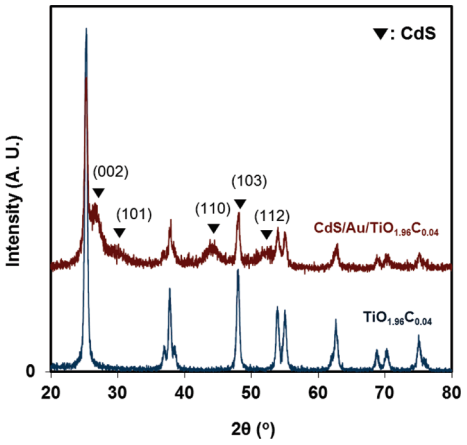

Figure 2. Crystalline structure of $TiO_{1.96}C_{0.04}$ and $CdS/Au/TiO_{1.96}C_{0.04}$ nanoparticles. $TiO_{1.96}C_{0.04}$ consists of only an anatase framework without any other crystalline phase, such as rutile or brookite, present. A typical XRD pattern for wurtzite-structured CdS was observed for the prepared photocatalysts, indicating the presence of CdS.

nanoparticles have only an anatase framework without any other crystalline phase, such as rutile or brookite. Peaks corresponding to Au were not observed in XRD patterns for $CdS/Au/TiO_{1.96}C_{0.04}$ due to the small amounts present and the size of the particles. In addition, a typical XRD pattern for wurtzite structured CdS (▼ marked) was found on the prepared photocatalysts with crystallographically preferred orientations, indicating the presence of CdS. UV−vis−DRS results permitted the band gap energy of the prepared semiconducting material to be estimated. The dark green powder absorbed large amounts of photons (Figure 5). Two shoulders (corresponding to regions I and II) were observed in the UV−vis−DRS of the $CdS/Au/TiO_{1.96}C_{0.04}$ sample. The drastic increase in its

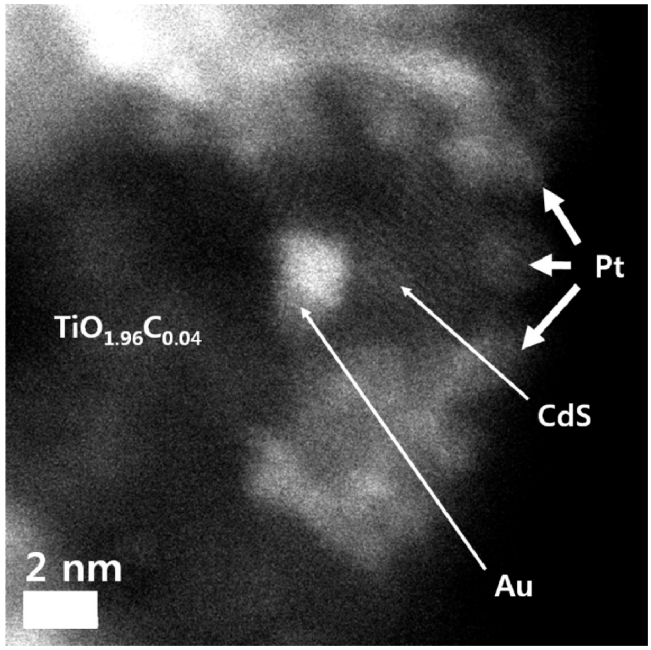

Figure 3. HAADF-STEM image of Pt/CdS/Au/$TiO_{1.96}C_{0.04}$ nanoparticles. Small Pt nanoparticles were observed on the CdS shell as bright spots.

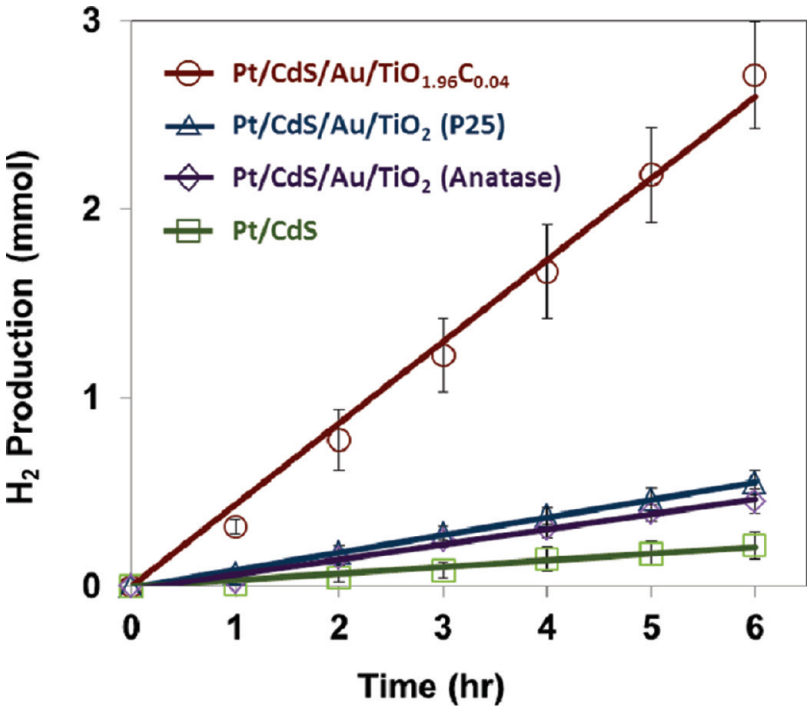

Figure 4. H_2 production *via* photocatalytic water-splitting. H_2 production of Pt/CdS/Au/$TiO_{1.96}C_{0.04}$, Pt/CdS/Au/TiO_2 (P25), Pt/CdS/Au/TiO_2 (anatase), and Pt/CdS under irradiation by visible light (using a wavelength longer than 420 nm).

absorbance at region I is caused by the presence of the CdS shell on the Au core. The value of E_g was estimated to be 2.3 eV, corresponding to CdS, by performing linear extrapolation from this shoulder. In addition, another shoulder (region II) was observed, which is related to $TiO_{1.96}C_{0.04}$. However determining the value of E_g from the presented UV–vis–DRS was not an easy task, because they are completely convoluted. Our previous research, however, indicated that $TiO_{1.96}C_{0.04}$ has an E_g of 2.6 eV.[30] The above findings show that wurtzite-structured CdS having an E_g of 2.3 eV was successfully constructed on the Au nanoparticles to form PS I, as evidenced by TEM, XRD, and UV–vis–DRS data.

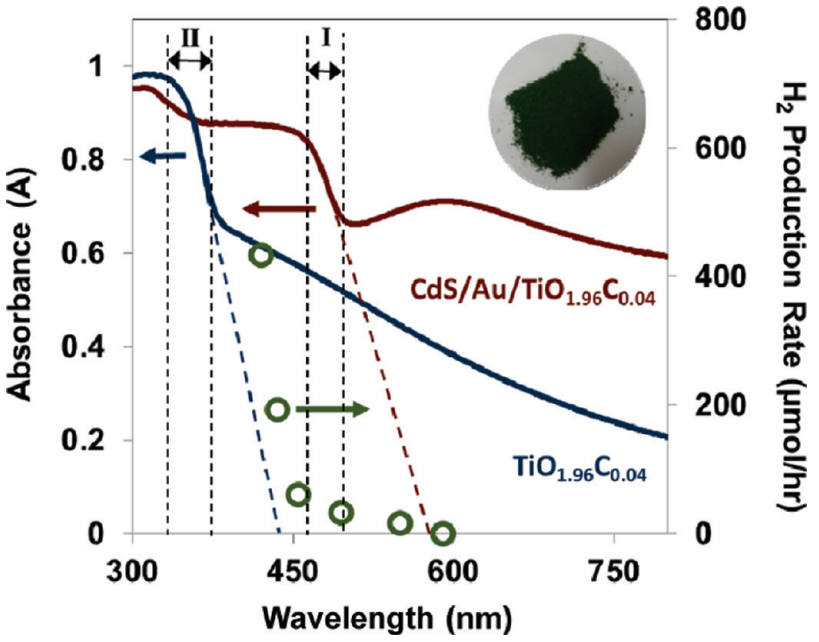

Figure 5. UV−vis absorbance of green CdS/Au/$TiO_{1.96}C_{0.04}$ powder and influence of light wavelength on H_2 evolution *via* water-splitting on Pt/CdS/Au/$TiO_{1.96}C_{0.04}$. One peak and two shoulders (region I and II) were observed in the UV−vis−DRS of the CdS/Au/$TiO_{1.96}C_{0.04}$ sample. The appearance of the peak is caused by surface plasmon of Au nanoparticles, consistent with the presence of deposited Au. The shoulder at region I is due to the presence of the CdS shell on the Au core. The value of E_g was estimated to be 2.3 eV, corresponding to CdS. The other shoulder was observed at region II, and is assigned to $TiO_{1.96}C_{0.04}$. Green open circles indicate the H_2 evolution rate for Pt/CdS/Au/$TiO_{1.96}C_{0.04}$ under the irradiation of visible light cut off each wavelength.

To investigate the performance of prepared catalysts, we carried out hydrogen evolution experiments *via* photocatalytic water-splitting. A small amount of Pt was deposited on the prepared samples as a cocatalyst for the reduction of protons, as described in previous reports.[6−8] The photodeposition method used UV light irradiated from 300 W Xe lamp to load the Pt cocatalyst. Inductively coupled plasma−atomic emission spectroscopy (ICP−AES) analyses indicated that 1 wt % Pt was deposited on each photocatalyst. HAADF-STEM analysis, which easily distinguishes between different materials in a very small dimension, was carried out to verify the presence of Pt nanoparticles on the CdS shell as cocatalyst for water-splitting (Figure 3). The images clearly show that they are relatively evenly deposited on the CdS shell with a uniform size and shape.

The time courses for H_2 production are presented in Figure 4. We prepared the following seven photocatalysts: Pt/CdS/Au/$TiO_{1.96}C_{0.04}$, Pt/CdS/Au/TiO_2 (P25), Pt/CdS/Au/TiO_2 (anatase), Pt/CdS, Pt/$TiO_{1.96}C_{0.04}$, Pt/TiO_2 (P25), and Pt/TiO_2 (anatase) to clarify the superiority of the Z-scheme mechanism under irradiation by visible light (of wavelength longer than 420 nm). Pt/TiO_2 (both P25 and anatase) and Pt/$TiO_{1.96}C_{0.04}$ did not produce any detectable amounts of H_2 fuel due to the low energy level of their conduction bands, which are close to the standard potential of H^+/H_2. This inhibits the transfer of photogenerated electrons at TiO_2 to H^+ ions. About 91.9 and 76.2 μmol h^{-1} of H_2 molecules (quantum efficiency, QE = 5.0 and 4.1) were generated by the Pt/CdS/Au/TiO_2 (P25) and Pt/CdS/Au/TiO_2 (anatase) catalysts under irradiation by visible light, respectively, despite the poor sensitivity of TiO_2 to visible light. This reductive performance can be attributed to the operation of only the CdS shell or CdS sensitized electrons. It can produce a larger amount of H_2 molecules than bulk Pt/CdS catalyst (34.6 μmol h^{-1}, QE = 1.9). On the other hand, Pt/CdS/Au/$TiO_{1.96}C_{0.04}$ generated 433.2 μmol h^{-1} of H_2 molecules (QE = 23.6), a much larger amount than Pt/CdS/Au/TiO_2. In this artificial Z scheme that mimics the natural photosynthesis system, electrons that are photogenerated at PS II under the irradiation of visible light were transferred to PS I through the Au core. These electrons then played an important role in reducing photogenerated holes at CdS, causing a decrease in the probability of charge recombination at PS I. Thus a higher amount of photogenerated electrons at PS I are available to participate in the reduction of protons. The successful realization of an all-solid-state Z-scheme mechanism under the irradiation of visible light led to an exceptional performance in the photocatalytic evolution of H_2 *via* water-splitting.

To verify how reaction progresses under the visible light with various wavelengths, we examined the effect of the wavelength of the visible light used on the rate of production of H_2. The rate of production of H_2 on Pt/CdS/Au/$TiO_{1.96}C_{0.04}$ tended to decrease drastically with an increase in wavelength cutoff, consistent with the extrapolation fitting line from the absorbance spectrum of $TiO_{1.96}C_{0.04}$ (Figure 5). These phenomena are

obviously caused by a decrease in the photocatalytic activities of PS II under the irradiation of visible light with a long wavelength. Moreover, Pt/CdS/Au/$TiO_{1.96}C_{0.04}$ generated 60.4 μmol h^{-1} of H_2 under the irradiation of pale green light with a longer wavelength than 455 nm, which roughly corresponds to the band edge of $TiO_{1.96}C_{0.04}$. This amount is similar to the 91.9 μmol h^{-1} of H_2 generated using light with a longer wavelength than 420 nm for Pt/CdS/Au/TiO_2. Visible light with a longer wavelength than 455 nm cannot activate PS II in the Pt/CdS/Au/$TiO_{1.96}C_{0.04}$ system, but only CdS (PS I) can produce exitons capable of reducing protons.

CONCLUSIONS

An artificial photosynthesis system mimicking the Z-scheme operation under visible light was successfully realized by combining two visible light sensitive photocatalysts, $TiO_{1.96}C_{0.04}$ and CdS. This combination enables the Z-scheme mechanism to be accomplished in one nanoparticle, and the production of photogenerated electrons having a sufficiently high potential to reduce protons with a much lower probability of charge recombination. Consequently, the system shows a highly efficient performance in H_2 generation *via* photocatalytic water-splitting under the irradiation of visible light. The findings reported herein indicate the potential for achieving photocatalytic hydrogen evolution *via* water-splitting. Further investigations to improve photocatalytic performance and explorations directed toward potential applications are currently in progress.

EXPERIMENTAL SECTION

Sample Preparation. $TiO_{1.96}C_{0.04}$ nanoparticles were synthesized by a gel−sol method. The procedure for preparing $TiO_{1.96}C_{0.04}$ nanoparticles was as follows. Titanium tetraisopropoxide (60 mL, Advanced Materials Institute Co. Ltd., 98%) was added to triethanolamine (54 mL, Sigma, 98%). Deionized water (DI water) was then added to give 400 mL of an aqueous solution. This solution (30 mL) was mixed with an aqueous solution of oleic acid (30 mL, 0.02 M). The pH of medium solution was controlled at pH 8 by adding nitric acid. This mixture was placed in a Teflon-lined autoclave and heated at 100 °C for 12 h to form a $Ti(OH)_4$ gel, which was then heated at 250 °C for 48 h, to give a brown-colored $TiO_{1.96}C_{0.04}$ precipitate. Organic residue and elemental carbon located on the surface of the $TiO_{1.96}C_{0.04}$ nanoparticles was completely removed by heating at 320 °C for 8 h under an atmosphere of air. Anatase-structured TiO_2 nanoparticles were synthesized following a procedure similar to that described above, except for the final heat treatment, which was performed at 450 °C for 8 h.

Au nanoparticles were deposited on the surface of $TiO_{1.96}C_{0.04}$ by the direct reduction of $AuCl^{4-}$ with $NaBH_4$. Brown-colored $TiO_{1.96}C_{0.04}$ powder (0.5 g) was well-dispersed in DI water (200 mL) through consecutive processes of ultrasonication for 1 h and rigorous stirring for 1 h. Chloroauric acid ($HAuCl_4$, 60 mmol) was introduced into this dispersion resulting in the deposition of 2 wt % of Au nanoparticles on the $TiO_{1.96}C_{0.04}$. After stirring for 30 min, 7.9 mL of a $NaBH_4$ aqueous solution (0.2 M) was added dropwise into the aqueous dispersion to reduce the Au^{3+} ions. Au/$TiO_{1.96}C_{0.04}$ was obtained after stirring for 3 h followed by centrifugation.

A hemispherical Au@CdS core−shell structure on $TiO_{1.96}C_{0.04}$ was produced by photodeposition. Sulfur (2 mmol) and $Cd(ClO_4)\cdot 6H_2O$ (8 mmol) was added to a ethanol suspension (200 mL) containing Au/$TiO_{1.96}C_{0.04}$. The suspension was irradiated with UV light for 12 h, giving a suspension changed from purple to dark green, indicating the formation of a CdS shell on the Au core. A Xe arc lamp (300 W, Oriel) was used as the light source for the UV light irradiation. After centrifuging and cleaning with ethanol several times, we prepared a suspension in methanol (100 mL) for the next procedure. For comparison, we synthesized CdS/Au/TiO_2 following the same procedure described above using commecial (P25, Degussa) and anatase TiO_2 instead of $TiO_{1.96}C_{0.04}$.

Pt nanoparticles were also loaded on the prepared samples by a photodeposition method as cocatalyst for water-splitting. We added $H_2PtCl_6\cdot 6H_2O$ (0.02 g) and triethylamine (4 mL) to the methanol suspension containing the photocatalyst. The resulting suspension was then irradiated with UV light for 14 h. Finally, the Pt-deposited photocatalyst was obtained after centrifugation.

Characterization of CdS/Au/$TiO_{1.96}C_{0.04}$. The shapes of the synthesized CdS/Au/$TiO_{1.96}C_{0.04}$ nanoparticles were examined by high-resolution transmission electron microscopy (HR-TEM, JEM 3010-JEOL, 300 kV) and high-angle annular dark-field scanning transmission electron microscopy (HAADF-STEM, JEM 2100F-JEOL, 200 kV). The microstructure was examined by X-ray diffracton (XRD, D/max-2500/PC-Rigaku) with Cu Kα radiation (wavelength = 0.154 nm) as the incident beam at 50 kV and 100 mA. Optical absorbance spectra were obtained by ultraviolet diffuse reflectance spectroscopy (UV-DRS, V670-Jasco). The atomic ratio of each component in CdS/Au/$TiO_{1.96}C_{0.04}$ was determined by inductively coupled plasma−atomic emission spectroscopy (ICP−AES, Optima-4300 DV-PerkinElmer).

Characterization of Photocatalytic Activities. Prior to photocatalytic hydrogen production, we examined the photocatalytic oxidation of the S^{2-} anion over $TiO_{1.96}C_{0.04}$, and TiO_2 (P25 and anatase). A total of 0.1 g of each powdered catalyst was suspended in 100 mL of an aqueous Na_2S solution (0.001 M) with vigorous stirring. A Xe arc lamp (300 W, Oriel) was used as the light source for irradiation with visible light. An optical filter (cutoff <420 nm, Edmund Optics) was used to eliminate UV radiation during the visible light experiments. The concentration of S^{2-} anions was measured using an ion selective electrode (ISE) meter (model 920, ThermoOrion) equipped with a sufide ion selective electrode (9616BNWP ionplus Sure-Flow Silver/Sulfide, Orion).

Photocatalytic hydrogen production *via* water-splitting was performed in a closed Pyrex glass reactor. For investigations of photocatalytic performance, each photocatalyst (0.15 g) was suspended in Na_2S (0.05 M) and Na_2SO_3 (0.1 M) aqueous solution (150 mL) under vigorous stirring. A Xe arc lamp was also used as the light source for irradiation with visible light for the photocatalytic reactions. All optical filters were supplied by Edmund Optics. A colored glass filter (cutoff <420, 435, 455, 495, and 550 nm) was used in the irradiation with various wavelengths of visible light during the water-splitting experiments. The amount of hydrogen produced was determined by gas chromatography (Acme6100-Young Lin), using a thermal conductivity detector (TCD). The quantum efficiency (QE) was estimated using the following equation,

$$\mathrm{QE} = \frac{2 \times \text{number of evolved } H_2 \text{ molecules}}{\text{number of incident photons}} \times 100$$

The number of incident photons was measured by a light power meter (Nova II, Ophir) equipped with a high power fan cooled thermal sensor (FL500A, Ophir). We assumed that all incident

photons are absorbed by the photocatalyst. Details of the method for calculating the number of incident photons is presented in the Supporting Information.

Acknowledgment. This research was supported by WCU (World Class University) program through the National Research Foundation of Korea funded by the Ministry of Education, Science and Technology (R31-10013), and the National Research Laboratory (NRL, 2000-N-NL-01-C-257) of the Korean Science and Engineering Foundation (KOSEF).

Supporting Information Available: Photocatalytic oxidation of S^{2-} anion under the irradiation of visible, and the calculation of the number of incident photons in detail. This material is available free of charge *via* the Internet at http://pubs.acs.org.

REFERENCES AND NOTES

1. O'Regan, B.; Grätzel, M. A Low-Cost, High-Efficiency Solar Cell Based on Dye-Sensitized Colloidal TiO_2 Films. *Nature* **1991**, *353*, 737–740.
2. Kamat, P. V. Quantum Dot Solar Cells. Semiconductor Nanocrystals as Light Harvesters. *J. Phys. Chem. C* **2008**, *112*, 18737–18753.
3. Fuke, N.; Hoch, L. B.; Koposov, A. Y.; Manner, V. W.; Werder, D. J.; Fukui, A.; Koide, N.; Katayama, H; Sykora, M. CdSe Quantum-Dot-Sensitized Solar Cell with ~100% Internal Quantum Efficiency. *ACS Nano* **2010**, *4*, 6377–6386.
4. Günes, S.; Neugebauer, H.; Sariciftci, N. S. Conjugated Polymer-Based Organic Solar Cells. *Chem. Rev.* **2007**, *107*, 1324–1338.
5. Fujishima, A.; Honda, K. Electrochemical Photolysis of Water at a Semiconductor Electrode. *Nature* **1972**, *238*, 37–38.
6. Osterloh, F. E. Inorganic Materials as Catalysts for Photochemical Splitting of Water. *Chem. Mater.* **2008**, *20*, 35–54.
7. Wang, X.; Maeda, K.; Thomas, A.; Takanabe, K.; Xin, G.; Carlsson, J. M.; Domen, K.; Antonietti, M. A Metal-free Polymeric Photocatalyst for Hydrogen Production from Water under Visible Light. *Nat. Mater.* **2009**, *8*, 76–80.
8. Maeda, K.; Domen, K. New Non-oxide Photocatalysts Designed for Overall Water Splitting under Visible Light. *J. Phys. Chem. C* **2007**, *111*, 7851–7861.
9. Walter, M. G.; Warren, E. L.; McKone, J. R.; Boettcher, S. W.; Mi, Q.; Santori, E. A.; Lewis, N. S. Solar Water Splitting Cells. *Chem. Rev.* **2010**, *110*, 6446–6473.
10. Chen, X.; Shen, S.; Guo, L.; Mao, S. S Semiconductor-Based Photocatalytic Hydrogen Generation. *Chem. Rev.* **2010**, *110*, 6503–6570.
11. Hahn, N. T.; Ye, H.; Flaherty, D. W.; Bard, A. J.; Mullins, C. B. Reactive Ballistic Deposition of α-Fe_2O_3 Thin Films for Photoelectrochemical Water Oxidation. *ACS Nano* **2010**, *4*, 1977–1986.
12. Bao, N.; Shen, L.; Takata, T.; Domen, K. Self-Templated Synthesis of Nanoporous CdS Nanostructures for Highly Efficient Photocatalytic Hydrogen Production under Visible Light. *Chem. Mater.* **2008**, *20*, 110–117.
13. Hu, C. -C.; Teng, H. Gallium Oxynitride Photocatalysts Synthesized from $Ga(OH)_3$ for Water Splitting under Visible Light Irradiation. *J. Phys. Chem. C* **2010**, *114*, 20100–20106.
14. Park, H.; Choi, W.; Hoffmann, M. R. Effects of the Preparation Method of the Ternary CdS/TiO_2/Pt Hybrid Photocatalysts on Visible Light-Induced Hydrogen Production. *J. Mater. Chem.* **2008**, *18*, 2379–2385.
15. Chen, J. -J.; Wu, J. C. S.; Wu, P. C.; Tsai, D. P. Plasmonic Photocatalyst for H_2 Evolution in Photocatalytic Water Splitting. *J. Phys. Chem. C* **2011**, *115*, 210–216.
16. Youngblood, W. J.; Anna Lee, S. -H.; Maeda, K.; Mallouk, T. E. Visible Light Water Splitting Using Dye-Sensitized Oxide Semiconductors. *Acc. Chem. Res.* **2009**, *42*, 1966–1973.
17. Sayama, K.; Mukasa, K.; Abe, R.; Abe, Y.; Arakawa, H. A New Photocatalytic Water Splitting System under Visible Light Irradiation Mimicking a Z-Scheme Mechanism in Photosynthesis. *J. Photochem. Photobiol. A* **2002**, *148*, 71–77.
18. Sasaki, Y.; Iwase, A.; Kato, H.; Kudo, A. The Effect of Co-Catalyst for Z-Scheme Photocatalysis Systems with an Fe^{3+}/Fe^{2+} Electron Mediator on Overall Water Splitting under Visible Light Irradiation. *J. Catal.* **2008**, *259*, 133–137.
19. Thampi, K. R.; Kiwi, J.; Grätzel, M. Methanation and Photomethanation of Carbon Dioxide at Room Temperature and Atmospheric Pressure. *Nature* **1987**, *327*, 506–508.
20. Roy, S. C.; Varghese, O. K.; Paulose, M.; Grimes, C. A. Toward Solar Fuels: Photocatalytic Conversion of Carbon Dioxide to Hydrocarbons. *ACS Nano* **2010**, *4*, 1259–1278.
21. Amao, Y.; Watanabe, T. Photochemical and Enzymatic Methanol Synthesis from HCO^{3-} by Dehydrogenases Using Water-Soluble Zinc Porphyrin in Aqueous Media. *Appl. Catal. B* **2009**, *86*, 109–113.
22. Morris, A. J.; Meyer, G. J.; Fujita, E. Molecular Approaches to the Photocatalytic Reduction of Carbon Dioxide for Solar Fuels. *Acc. Chem. Res.* **2009**, *42*, 1983–1994.
23. Lewerenz, H. J.; Heine, C.; Skorupska, K.; Szabo, N.; Hannappel, T.; Vo-Dinh, T.; Campbell, S. A.; Klemm, H. W.; Muñoz, A. G. Photoelectrocatalysis: Principles, Nanoemitter Applications and Routes to Bio-inspired Systems. *Energy Environ. Sci.* **2010**, *3*, 748–760.
24. Barber, J. Photosynthetic Energy Conversion: Natural and Artificial. *Chem. Soc. Rev.* **2009**, *38*, 185–196.
25. Sun, L.; Hammarström, L.; Åkermark, B.; Styring, S. Towards Artificial Photosynthesis: Ruthenium-Manganese Chemistry for Energy Production. *Chem. Soc. Rev.* **2001**, *30*, 36–49.
26. Berg, J. M.; Tymoczko, J. L.; Stryer, L. *Biochemistry*, 5th ed.; W. H. Freeman and Company: New York, 2006.
27. Conlan, B. Designing Photosystem II: Molecular Engineering of Photocatalytic Proteins. *Photosynth. Res.* **2008**, *98*, 687–700.
28. Tada, H.; Mitsui, T.; Kiyonaga, T.; Akita, T.; Tanaka, K. All-Solid-State Z-Scheme in CdS-Au-TiO_2 Three-Component Nanojunction System. *Nat. Mater.* **2006**, *5*, 782–786.
29. Yun, H. J.; Lee, H.; Joo, J. B.; Kim, N. D.; Kang, M. Y.; Yi, J. Facile Preparation of High Performance Visible Light Sensitive Photocatalysts. *Appl. Catal. B* **2010**, *94*, 241–247.
30. Yun, H. J.; Lee, H.; Joo, J. B.; Kim, N. D.; Yi, J. Tuning the Band-Gap Energy of $TiO_{2-x}C_x$ Nanoparticle for High Performance Photocatalyst. *Electrochem. Commun.* **2010**, *12*, 769–772.